

What are the Magic Clusters Observed in Graphene Chemical Vapor Deposition (CVD) Growth?

Junfeng Gao, and Feng Ding^{1,2*}

Beijing Computational Science Research Center, Beijing, 100084, China.

Institute of Textiles and Clothing, Hong Kong Polytechnic University, Hong Kong, China.

To improve atomically controlled chemical vapor deposition (CVD) growth of graphene, understanding the evolution from various carbon species to a graphene nuclei on various catalyst surfaces is essential. Experimentally, an ultra-stable carbon cluster on Ru(0001), Rh(111) surfaces was observed, while its structure and formation process were still under highly debate. Using *ab initio* calculations and kinetic analyses, we disclosed a specific type of carbon clusters, composed of a C₂₁ core and a few dangling C atoms around, were exceptional stable in the size range from 21 to 27. The most stable one of them, an isomer of C₂₄ characterized as three dangling C atoms attached to the C₂₁ (denoted as C₂₁-3C), is the most promising candidate for the experimental observation. The ultra-stability of C₂₁-3C originates from both the stable core and the appropriate passivation of dangling carbon atoms by the catalyst surface.

Keywords: Graphene; chemical vapor deposition; density functional theory, C₂₁H₁₂ sumanene.

Due to the recorded electron/hole mobility,^[1] extremely high thermal conductivity^[2, 3] and superior mechanical performance^[4, 5], the two-dimensional graphene was broadly studied for many applications, such as ultrafast transistor,^[6, 7] transparent and flexible electrode,^[8] etc.^[9]

Among the known methods of graphene synthesis, the chemical vapor deposition (CVD) is the best way to achieve high-quality single or few graphene layers with macroscopic area (up to 1000 inch²) at a reasonable price, and therefore it was extensively explored both experimentally and theoretically.^[10-28] In a CVD experiment, the transition metal surface, on which graphene is formed by the self-assembly of the dissociated or deposited C atoms or radicals, plays a crucial role. To date, a cornucopia of transition metals, such as Ru,^[11, 29] Rh,^[30] Ir,^[11] Cu,^[17, 21] Ni,^[31] Pt^[23], Au^[32] and their metal alloys (i. e. Ni/Mo^[19] and Ni/Cu^[20]) were proved to be suitable for CVD of graphene.

The first stage in the CVD growth of graphene—the nucleation of graphene on the catalyst surface determines both the density of nuclei and the concentration of grain boundaries in the final product. Therefore nucleation of graphene has been intensively studied recently.^[10-18] Theoretically, the evolution of C clusters and the size-dependent C formations on the catalyst surface have been investigated to determine the nucleation barrier and size of nuclei under various growth conditions.^[13] Previous theoretical explorations have shown that, by carefully optimizing the experimental condition, the size of nuclei can be controlled between N=20–100.^[13-15] Therefore the structures and stabilities of carbon clusters in this range are crucial for understanding the graphene nucleation.

For graphene nucleation on Ru(0001) and Rh(111) surfaces, an astonishing experimental observation is the existence of ultra-stable carbon clusters of ~1 nm in diameter.^[33-35] Although different feedstock (e.g., C₂H₄,^[33, 34] C₁₂H₂₄^[33] and C₆₀^[35]) were used in the graphene synthesis, nearly all the decomposed C atoms on the catalyst terrace were observed in the form of the uniformed ultra-stable clusters at the temperature range of 870 K-1000 K, indicating that this cluster is highly superior to others in a very large size range. Mimicking the terminology of cluster science, we hereafter call them “magic clusters”.

However, due to the high curvature near edge of the cluster and the influence of metal surface, scanning tunneling microscope (STM) was unable to disclose the precise atomic structure of the magic cluster. As its size is close to that of a coronene molecule (C₂₄H₁₂), the magic carbon cluster was once suspected to be the dehydrogenated coronene, i.e. the C₂₄ with seven 6-membered-rings, namely 7-6MRs^[36] or 7-C6.^[33, 34] Latterly, by systemically searching the sp² hybridized C clusters on various metal surfaces, we suggested that a closed

core-shell isomer of C_{21} , which was characterized as one hexagon surrounded by three hexagons and three pentagons alternatively, was much more stable than the 7-6MRs. Therefore, the C_{21} isomer was highly considered as the observed magic cluster.^[36]

In this manuscript, via density functional theory (DFT) calculations, we presented a new ultra-stable isomer of C_{24} , which has the core of the aforementioned C_{21} and three dangling C atoms attached to the three pentagons (denoted as C_{21} -3C). The C_{21} -3C, with much lower formation energy than the C_{21} and 7-6MRs, corresponds the global minimum and has the dominate population in a large cluster size range, $20 \leq N \leq 30$ on the Ru(0001), Rh(111) surfaces. This study proposed a more probable candidate for the experimentally observed magic cluster in graphene CVD growth and explained its significant stability on both Ru(0001) and Rh(111) surfaces.

To demonstrate the stability and formation of the C_{21} -3C isomer, we proposed an isomerization from the 7-6MRs to C_{21} -3C on the Ru(0001) surface. Details of DFT calculations are in Supporting information 2(S2). Figure 1a shows the transformation from the 7-6MRs to the C_{21} -3C via the successive rearrangement of the three edge C-C bonds. The first bond rotation leads to a meta-stable structure with 1.32 eV higher in energy. After that, the second bond rotation becomes -0.08 eV lower than 7-6MRs in energy, implying this structure is thermodynamically more stable than the 7-6MRs. With the third bond rotation, the energy of the final C_{21} -3C is greatly reduced to -1.99 eV eventually. Such a remarkable energy reduction implies that the C_{21} -3C isomer is much more stable than the initial 7-6MRs. With these in hand, the population ratio of 7-6MRs to C_{21} -3C in thermal equilibrium can be estimated by

$$P_{7-6MR}/P_{C_{21}-3C} = \exp(-1.99 \text{ eV}/k_B T) = 10^{-11} \quad (1)$$

at the experimental temperature of 900 K, where k_B is the Boltzmann constant and T is the temperature. Besides, isomerization from the 7-6MRs to C_{21} -3C should be easily occurred at the experimental temperature of ~ 900 K as the energy barrier for a C-C bond rotation is only 1.38 eV (see Figure S3a), which slightly lower than the bond rotation of graphene zigzag edge on Co surfaces.^[22] These results imply the observation of the 7-6MRs via dehydrogenated coronene on Ru(0001) surface is nearly impossible.^[33]

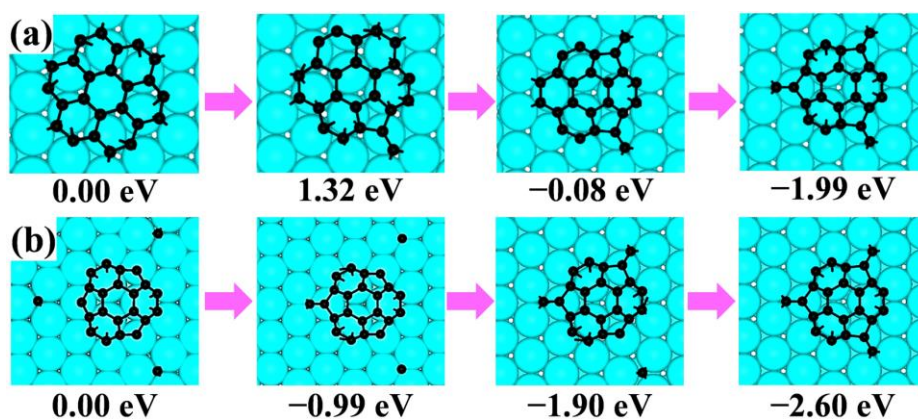


Figure 1. a) The isomerization from the 7-6MR to the C₂₁-3C of C₂₄ on Ru(0001) surface; b) a core-shelled C₂₁ adsorbs three carbon adatoms and becomes the C₂₁-3C on the Ru(0001) surface.

Next, let's consider the stability of the C₂₁-3C in relative to the previous proposed C₂₁ on the Ru(0001) surface.^[36] A C₂₁-3C can be formed by a C₂₁ adsorbing three more C atoms from the catalyst surface (Figure 1b). The barriers of these atomic adsorptions are extremely low, less than 1.0 eV (see Figure S3b), and energy reductions are -0.99 eV, -1.90 eV and -2.6 eV, respectively. Considering the formation energy of a C monomer on the catalyst surface is about 0.55 eV higher than graphene, the formation energy of the C₂₁-3C is ~ 1.0 eV lower than the core-shelled C₂₁, the most stable cluster shown in the previous study.^[36] Thereby, if there are sufficient C monomers on the catalyst surface, up to $[1 - \exp(-2.6 \text{ eV}/k_B T)] = \sim 99.99\%$ of the core-shelled C₂₁ will be quickly transformed into the branched C₂₁-3C in the temperature range of 870 K–1000 K easily.

Above analysis clearly demonstrated the superior of branched C₂₁-3C over the dehydrogenated 7-6MRs and the core-shelled C₂₁. In order to understand the ultra-stability of the C₂₁-3C on the catalyst surface, let's exam its structural and electronic properties.

Both the C₂₁ and the C₂₁-3C have 9 active edge atoms. There is one dangling bond on each edge atom of the hexagon and two dangling bonds on each of the pentagon (for C₂₁) or the dangling carbon atom (for C₂₁-3C), thereby both C₂₁ and C₂₁-3C have 12 dangling bonds (see Figure 2a, d). However, the arrangement of paired dangling bonds on the edge of pentagon of C₂₁ is different from that on the dangling C atom of C₂₁-3C. On the edge of a pentagon, the C atom tends to be *sp*³ hybridized and the four σ bonds tends to be tetrahedrally distributed in space. As a consequence, one dangling bond on the edge of a pentagon of C₂₁ flips upwards and thus was not efficiently passivated by the metal surface as evidenced by the differential charge densities near the edge atom (the red dangling bonds of Figure 2b-c) and

Figure S4). For only one dangling bond can be passivated by the metal surface, the edge C atom of the pentagon locates on the top of a metal atom.

Different from C_{21} , a dangling atom of C_{21} -3C is sp^2 hybridized with one double bond and two dangling bonds according to the analysis of differential charge densities (Figure 2e). The arrangement of the two dangling bonds tends to be in the same plane of the tilted pentagon as the characteristic of the sp^2 C network (see Figure 2d). As a consequence, all edge dangling bonds can be effectively passivated by the metal surface. To passivate both dangling bonds efficiently, all the three dangling atoms of the C_{21} -3C locate near hollow and bridge sites of the metal surface as can be clearly seen in Figure 2e, 2i and Figure S4. The length of outer-most C-C bond of C_{21} -3C is about 1.44 Å.

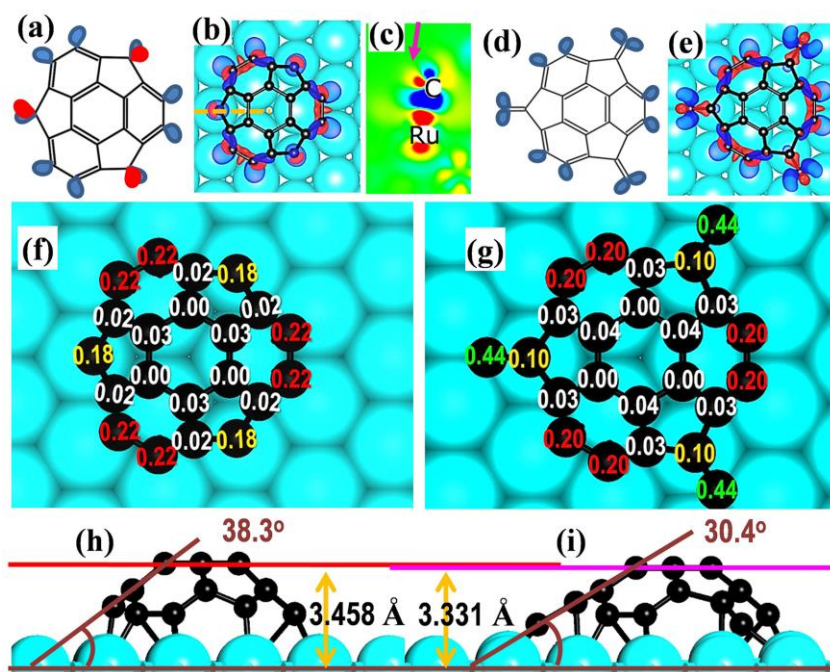


Figure 2. The schematics of dangling bonds of a) C_{21} and d) C_{21} -3C; the top view of differential charge densities of b) C_{21} and e) C_{21} -3C on Ru(0001) surface; c) the cross section view of the differential charge densities of the C_{21} @Ru(0001), the arrow points to the unpassivated dangling bond of the edge C atom; Bader charge analyses (in |e|) of f) C_{21} and g) C_{21} -3C on Ru(0001) surface; h-i) the optimized C_{21} and C_{21} -3C structures on the Ru(0001) surface.

Above analyses explicitly explained the high stability of C_{21} -3C in relative to the C_{21} was stemmed from the more effective passivation of dangling atoms on the catalyst surface. As calculated in previous study,^[36] the binding energies of C_{21} on Ru(0001), Rh(111), Ir(111) surfaces were 16.9 eV, 18.1 eV and 17.6 eV, respectively, which were significantly larger than the core-shelled C_{20} and 7-6MRs. Analyses with same method showed that the binding

energies of C₂₁-3C were further increased to 22.5 eV, 23.1 eV and 21.9 eV on these metal surfaces, respectively, which were 5.6 eV, 7.0 eV and 4.3 eV higher than those of C₂₁ (Table S6), although both configurations possessed the same number of active edge atoms. The very large binding energies further validated the efficient passivation of the three dangling atoms of the C₂₁-3C.

The stronger binding between the C₂₁-3C and catalyst surface than C₂₁ is also verified from the Bader charge transfer analysis. As shown in Figure 2f-g, one can see the total charge transfer from the metal to the C₂₁ is about 2 |e|, which is much smaller than that from the metal to C₂₁-3C, ~ 3 |e|. The difference is from the edge of the pentagons, where the charge transferred to an edge atom of a pentagon of C₂₁ is about 0.18 |e| while transferred to a dangling C atom of C₂₁-3C is about 0.44 |e|.

The height of the experimentally observed magic carbon cluster is ~1 Å higher than coronene on the catalyst surface.^[34] As shown in Figure 2h-i and Table S5, the height of C₂₁-3C is very close to that of C₂₁, which was proved about 1.23 Å higher than that of coronene.^[36] That is the height of C₂₁-3C is about 1.0~1.1 Å higher than coronene on catalyst surface, agreeing well with the experimental observation.^[34]

Now, let's consider the stability of the C₂₁-3C on metal surface from the point view of aromaticity. There are two typical nonplanar π -conjugated polycyclic aromatic hydrocarbon (PAH) molecules of the similar size, C₂₀H₁₀ (corannulene, synthesized in 1991^[37]) and C₂₁H₁₂ (sumanene, synthesized in 2003^[38]), and both were extensively studied before.^[39-43] As the C_{5v} symmetry of C₂₀ is different from that of the Ru(0001) surface, C₂₀ on the Ru(0001) surface is less stable than C₂₁. In comparison with the C₂₁, the C₂₁-3C on Ru(0001) have very similar bonding situation with sumanene (see Figure S6 and Table S6 for detailed discussion). They both have very similar bond angle of a pentagon (~103°) and the bond lengths difference in the hexagons in a C₂₁-3C on Ru(0001) is only 0.014 Å, which is even smaller than that of sumanene (0.046 Å).^[44] This implies that C₂₁-3C on metal surface can be viewed as a typical nonplanar π -conjugated aromatic C cluster.^[42, 44] In contrast, the C₂₁ on Ru surface has much larger bond angle on its pentagon (~ 107°) and bond length difference in its hexagons. It's also worth to note that the C₂₁-3C can be viewed as derivative of the extended π -conjugated sumanene as shown in Figure S6e and Ref. 45.

Moreover, the simulated STM image of the C₂₁-3C cluster on Ru(0001) is also in good agreement with the experimental ones (see Figure S7).^[33, 35] It is interesting that the simulated STM image of C₂₁ is also very close to the experimental ones.^[36] This is attributed to the

invisibility of the three dangling atoms due to their lower positions on the metal surface (Figure 2i). Same as that on Ru(0001) surface, the STM images of C_{21} and C_{21-3C} on Rh(111) and Ir(111) surfaces (Figure S8) are very similar to each other.^[34]

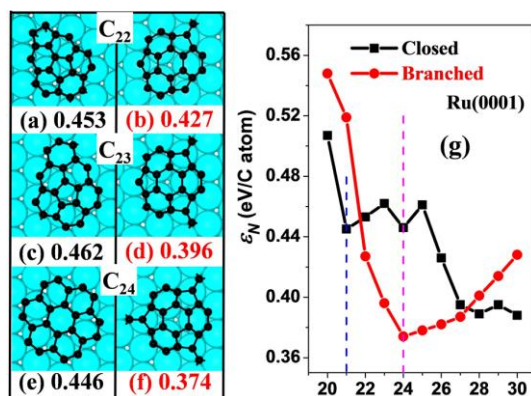


Figure 3. The most stable core-shell sp^2 network and branched C_N ($N = 22, 23, 24$) clusters on Ru(0001) surface (left panel) and the formation energies ϵ_N (in eV/C atom) of the most stable C_N ($N=20\sim 30$) clusters of each type on the Ru(0001) surface.

With above compelling evidences and analyses, the C_{21-3C} is expected to be the observed magic cluster in graphene CVD growth. As shown in previous study, the C_{21} has very similar stability with the 7-6MR isomer on Ru(0001) and Rh(111) surfaces, and thus it corresponds a local minimum in the size range of $N < 24$.^[36] How is the stability of the C_{21-3C} in relative to C_{21} and others? As shown in Figure 3, another two carbon clusters with one and two dangling edge atoms, namely C_{21-1C} (Figure 3b) and C_{21-2C} , respectively (Figure 3d), are also very stable. In order to fully address the stability of C_{21-3C} and its role of graphene nucleation, we systematically explored two series of C clusters, (i) those are composed of pentagons and hexagons only as studied previously^[13, 14, 18, 36] and (ii) those with one or a few dangling C atoms attached to the pentagons of the C_{21} core, on three catalyst surfaces—Ru(0001), Rh(111) and Ir(111). The most stable structures and corresponding formation energies of the clusters on Ru(0001), Rh(111) and Ir(111) surface were shown in Figure 3g, S9, S10 and S11, respectively. Besides, in order to find the lowest-energy structures in this regime, many different isomers were also considered (for example, some explored structures of C_{24} , C_{28} , C_{29} and C_{30} are shown in the Figure S12).

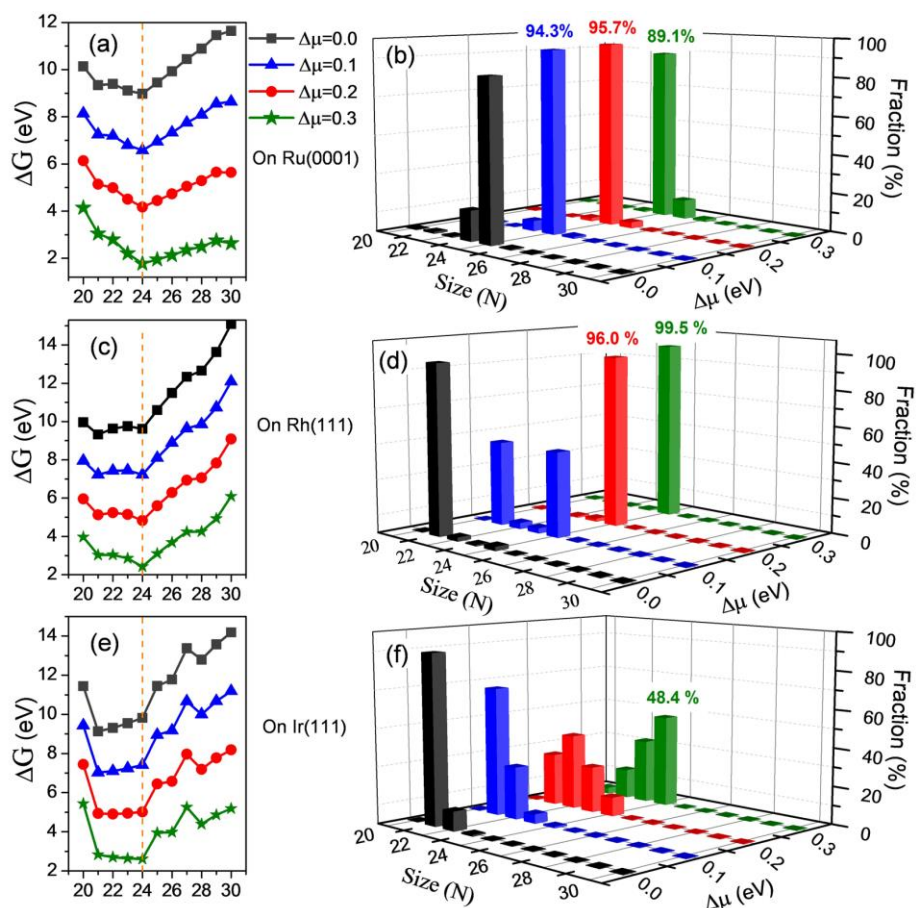


Figure 4. The Gibbs free energies and populations of C_N ($20 \leq N \leq 30$) clusters under different condition of graphene growth (denoted by the chemical potential difference between feedstock and graphene, $\Delta\mu=0.0, 0.1, 0.2$ and 0.3 eV) on a, b) Ru(0001); c, d) Rh(111), and e, f) Ir(111) surfaces, respectively.

For C_N on all the three catalyst surfaces, in the explored cluster size region ($20 \leq N \leq 30$), the C_{21-3C} represents a global minimum (see Figure 3g). On Ru(0001) surface, the formation energy per C atom of C cluster keep dropping from $N=20$ to $N=24$ and then keep rising from $N=24$ to $N=30$. This characteristic makes C_{21-3C} a deep global minimum in the size range of $20 \leq N \leq 30$. Although C_{21} and 7-6MRs also correspond two local minima in the energy curve of the core-shell clusters (vertical dash lines in Figure 3g),^[36] their formation energies are much higher than the branched C clusters on Ru(0001). This means that the branched C clusters possess the highest stability in the vicinity of size range of $N=24$ on Ru(0001) surface. It is important to note that the C clusters on both Rh(111) and Ir(111) surfaces exhibit very similar characteristics as that on Ru(0001) (Figure S9-11), implying that the above analyses may be universal for graphene CVD growth on metal surfaces.

Above analyses demonstrate that the branched C_{21-3C} isomer is superior in a large size region. To quantify the population of the C_{21-3C} cluster on metal surface under different

growth condition, let's introduce the chemical potential difference between the C atom in feedstock and in graphene on the catalyst surface, $\Delta\mu$. According to the classical theory of crystal nucleation,^[46] the population of a cluster can be estimated by

$$P_N = \exp(-\Delta G/kT), \quad (2)$$

where $\Delta G = E_N - N \times \Delta\mu$ is the Gibbs free energy and $E_N = N \times \epsilon_N$ is the total formation energy of cluster C_N . The calculated ΔG and normalized fraction P_N in the size range $20 \leq N \leq 30$ with $\Delta\mu = 0.0, 0.1, 0.2$ and 0.3 eV are shown in Figure 4, respectively. The kinetic stability of the clusters on the three catalyst surfaces is presented as following:

(i) On the Ru(0001) surface, the Gibbs free energy of the C_{21-3C} cluster is a deep local minimum in a large range of $\Delta\mu$ (Figure 4a). Due to the exceptional stability, the population of the C_{21-3C} always dominate in the explored size range (>89%) (Figure 4b).

(ii) On the Rh(111) surface, the C_{21} has the lower formation energy than C_{21-3C} at $\Delta\mu = 0.0$ eV, but when $\Delta\mu$ becomes slightly larger, i.e., $\Delta\mu > 0.2$ eV (common condition), the C_{21-3C} becomes more stable than C_{21} (Figure 4c). Thus the dominating of C_{21-3C} can be only observed in the range of $\Delta\mu \geq 0.2$ eV (Figure 4d).

(iii) On the Ir(111) surface, the small clusters, C_{21} , branched C_{22} and C_{23} are more stable than the C_{21-3C} in the range of $\Delta\mu < 0.2$ eV (Figure 4e). The dominating clusters is C_{21} at $\Delta\mu = 0.0$ eV but no dominating clusters until $\Delta\mu > 0.3$ eV (Figure 4f).

Above analyses indicate that the probability of observing the magic cluster on the three metal surfaces follows the order of Ru(0001) > Rh(111) > Ir(111). Such a trend is in perfect agreement with the known experimental facts. Experimentally, most reported magic clusters were on the Ru(0001),^[33, 35] and a few were on the Rh(111)^[35]. Although Ir(111) was considered as a very similar catalyst surface to Rh(111) and Ru(0001) for graphene growth, there's no uniformed C clusters on it.^[47]

In summary, using DFT calculations, we systemically investigated the stability of C_N clusters ($20 \leq N \leq 30$) on Ru(0001), Rh(111) and Ir(111) surfaces. Our study revealed a new type of ultra-stable carbon clusters—branched sp^2 carbon networks. The most stable one of them, C_{21-3C} , was predicated to be the experimentally observed magic cluster in graphene CVD growth on both Ru(001) and Rh(111) surfaces by stability and population analyses. Besides, we also successfully explained why the uniformed magic sized cluster only can be seen on Ru(0001) and Rh(111) surfaces but not on Ir(111) surface. This study provided a deep insight into the nucleation of graphene in the CVD growth processes and the formation mechanism of magic sized clusters might be used for the synthesis of graphene quantum dots.

Acknowledgements

We thank Prof. Zhenyang Lin of HKUST for useful discussion and acknowledge the supported by National Natural Science Foundation of China (No. 11304008), Development Fund of China Academy of Engineering Physics (No. 2013B0302056) and China Postdoctoral Science Foundation (No. 2014T70030, 2013M530019). The work was carried out at National Supercomputer Center in Tianjin, and the calculations were performed on TianHe-1(A).

- [1] A. K. Geim, K. S. Novoselov, *Nat. Mater.* **2007**, 6, 183-191.
- [2] A. A. Balandin, S. Ghosh, W. Bao, I. Calizo, D. Teweldebrhan, F. Miao, C. N. Lau, *Nano Lett.* **2008**, 8, 902-907.
- [3] A. A. Balandin, *Nat. Mater.* **2011**, 10, 569-581.
- [4] C. Lee, X. Wei, J. W. Kysar, J. Hone, *Science* **2008**, 321, 385;
- [5] Y. Liu, B. Xie, Z. Zhang, Q. Zheng, Z. Xu, *J. Mech. Phys. Solids* **2012**, 60, 591-605.
- [6] D. Wei, Y. Lu, C. Han, T. Niu, W. Chen, A. T. S. Wee, *Angew. Chem. Int. Ed.* **2013**, 52, 14121-14126.
- [7] Q. Yuan, H. Hu, J. Gao, F. Ding, Z. Liu, B. I. Yakobson, *J. Am. Chem. Soc.* **2011**, 133, 16072-16079.
- [8] H. Wang, K. Sun, F. Tao, D. J. Stacchiola, Y. H. Hu, *Angew. Chem. Int. Ed.* **2013**, 52, 9210-9214.
- [9] C. N. R. Rao, A. K. Sood, K. S. Subrahmanyam, A. Govindaraj, *Angew. Chem. Int. Ed.* **2009**, 48, 7752-7777.
- [10] X. Li, W. Cai, L. Colombo, R. S. Ruoff, *Nano Lett.* **2009**, 9, 4268-4272;
- [11] E. Loginova, N. C. Bartelt, P. J. Feibelman, K. F. McCarty, *New J. Phys.* **2009**, 11, 063046.
- [12] H. Chen, W. Zhu, Z. Zhang, *Phys. Rev. Lett.* **2010**, 104, 186101;

- [13] J. Gao, J. Yip, J. Zhao, B. I. Yakobson, F. Ding, *J. Am. Chem. Soc.* **2011**, 133, 5009-5015.
- [14] J. Gao, Q. Yuan, H. Hu, J. Zhao, F. Ding, *J. Phys. Chem. C* **2011**, 115, 17695-17703.
- [15] W. Zhang, P. Wu, Z. Li, J. Yang, *J. Phys. Chem. C* **2011**, 115, 17782-17787.
- [16] P. Wu, H. Jiang, W. Zhang, Z. Li, Z. Hou, J. Yang, *J. Am. Chem. Soc.* **2012**, 134, 6045-6051.
- [17] T. Niu, M. Zhou, J. Zhang, Y. Feng, W. Chen, *J. Am. Chem. Soc.* **2013**, 135, 8409-8414.
- [18] P. Wu, W. Zhang, Z. Li, J. Yang, *Small* **2014**, 2136-2150.
- [19] B. Dai, L. Fu, Z. Zou, M. Wang, H. Xu, S. Wang, Z. Liu, *Nat. Commun.* **2011**, 2, 522.
- [20] X. Liu, L. Fu, N. Liu, T. Gao, Y. Zhang, L. Liao, Z. Liu, *J. Phys. Chem. C* **2011**, 115, 11976-11982.
- [21] J. D. Wood, S. W. Schmucker, A. S. Lyons, E. Pop, J. W. Lyding, *Nano Lett.* **2011**, 11, 4547-4554.
- [22] J. Gao, J. Zhao, F. Ding, *J. Am. Chem. Soc.* **2012**, 134, 6204-6209.
- [23] L. Gao, et al., *Nat. Commun.* **2012**, 3, 699.
- [24] Z. Li, W. Zhang, X. Fan, P. Wu, C. Zeng, Z. Li, X. Zhai, J. Yang, J. Hou, *J. Phys. Chem. C* **2012**, 116, 10557-10562.
- [25] G.-H. Lee, et al., *Science* **2013**, 340, 1073-1076.
- [26] A. M. Lewis, B. Derby, I. A. Kinloch, *ACS Nano* **2013**, 7, 3104-3117.
- [27] X. Zhang, L. Wang, J. Xin, B. I. Yakobson, F. Ding, *J. Am. Chem. Soc.* **2014**, 136, 3040-3047.
- [28] T. Ma, W. Ren, X. Zhang, Z. Liu, Y. Gao, L.-C. Yin, X.-L. Ma, F. Ding, H.-M. Cheng, *Proc. Natl. Acad. Sci. U.S.A.* **2013**, 110, 20386-20391.
- [29] H. Zhang, Q. Fu, Y. Cui, D. Tan, X. J. Bao, *Phys. Chem. C* **2009**, 113, 8296-8301.
- [30] B. Wang, M. Caffio, C. Bromley, H. Früchtl, R. Schaub, *ACS Nano* **2010**, 4, 5773-5782.

- [31] Y. Zhang, L. Gomez, F. N. Ishikawa, A. Madaria, K. Ryu, C. Wang, A. Badmaev, C. Zhou, *J. Phys. Chem. Lett.* **2010**, 1, 3101-3107.
- [32] S. Nie, N. C. Bartelt, J. M. Wofford, O. D. Dubon, K. F. McCarty, K. Thürmer, *Phys. Rev. B* **2012**, 85, 205406.
- [33] Y. Cui, Q. Fu, H. Zhang, X. Bao, *Chem. Comm.* **2011**, 47, 1470-1472.
- [34] B. Wang, X. Ma, M. Caffio, R. Schaub, W.-X. Li, *Nano Lett.* **2011**, 11, 424-430.
- [35] J. Lu, P. S. E. Yeo, C. K. Gan, P. Wu, K. P. Loh, *Nat. Nano.* **2011**, 6, 247-252.
- [36] Q. Yuan, J. Gao, H. Shu, J. Zhao, X. Chen, F. Ding, *J. Am. Chem. Soc.* **2011**, 134, 2970-2975.
- [37] L. T. Scott, M. M. Hashemi, D. T. Meyer and H. B. Warren, *J. Am. Chem. Soc.* **1991**, 113, 7082.
- [38] H. Sakurai, T. Daiko and T. Hirao, *Science*, **2003**, 301, 1878.
- [39] G. N. Sastry, E. D. Jemmis, G. Mehta and S. R. Shah, *J. Chem. Soc., Perkin Trans.* **1993**, 2, 1867.
- [40] U. D. Priyakumar and G. N. Sastry, *J. Phys. Chem. A* **2001**, 105, 4488.
- [41] T. Amaya, S. Seki, T. Moriuchi, K. Nakamoto, T. Nakata, H. Sakane, A. Saeki, S. Tagawa and T. Hirao, *J. Am. Chem. Soc.* **2009**, 131, 408.
- [42] T. Amaya and T. Hirao, *Chem. Commun.* **2011**, 47, 10524.
- [43] S. Armaković, S. J. Armaković, J. P. Šetrajčić, *Int. J. Hydrogen Energ.* **2013**, 38, 12190.
- [44] H. Sakurai, T. Daiko, H. Sakane, T. Amaya and T. Hirao, *J. Am. Chem. Soc.* **2005**, 127, 11580.
- [45] T. Amaya, K. Mori, H.-L. Wu, S. Ishida, J. Nakamura, K. Murata, T. Hirao, *Chem. Commun.* **2007**, 1902.

[46] I. V. Markov, *Crystal Growth for Beginners: Fundamentals of Nucleation, Crystal Growth and Epitaxy, 2nd ed.*; World Scientific Publishing Co. Pte. Ltd.: Singapore, **2003**.

[47] J. Coraux, et al., *New J. Phys.* **2009**, 11, 023006.